Distinguishing Volcanic and Fluvial Activity in Mangala Valles, Mars via Geomorphic Mapping

A. L. Keske[1], C. W. Hamilton[2], A. S. McEwen[2], I. J. Daubar[2],
[1]School of Earth and Space Exploration, Arizona State University, Tempe AZ, 85281 (alkeske@asu.edu), [2]Lunar and Planetary Laboratory, University of Arizona, Tucson AZ, 85721.

Summary: A new mapping–based study of the Mangala Valles outflow system aims to characterize its geologic history using cratering statistics, geomorphic surface mapping, and stratigraphic relations. Crater counts performed at 29 locations throughout the area have allowed us to construct a timeline involving the occurrence of at least three major volcanic phases and at least two major fluvial events in the Middle to Late Amazonian. These results are consistent with a geologic history consisting of recurrent phases of valley flooding alternating with or in concert with phases of volcanic activity in the valles. Such repeated episodic behavior suggests continual aquifer and magma chamber replenishment during an extended period of time within the subsurface of the Mangala Valles region.

Background

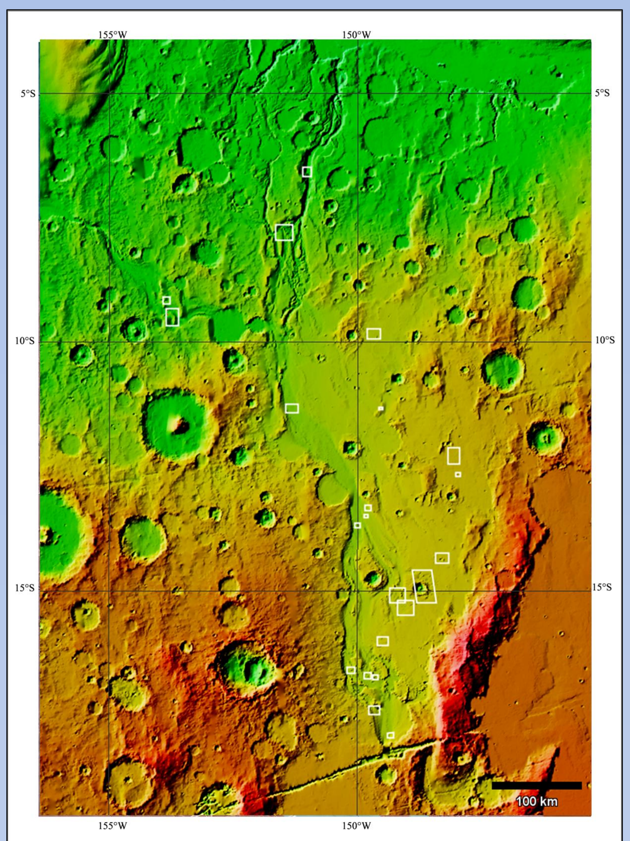

The 900-km long Mangala Valles originates at Mangala Fossa, part of the Memnonia Fossae graben system. Large-scale channel landforms in major outflow regions on Mars such as Kasei, Ares, Tiu, Simund, and Mangala Valles have been compared to the channeled scablands of the Pacific Northwest, leading to general acceptance that these valleys were carved by water during "megaflooding" events *[19,20,21,22,23]*. However, observations of volcanic deposits present on the channel floors in some of these regions have led to an alternative hypothesis suggesting that large martian outflow regions such as Mangala Valles were instead carved by vast volumes of lava *[5,6]*. Alternate hypotheses for Mangala Valles include the exposure of previously buried volcanic material by flooding *[2,4]*, fluvial activity followed by glacial activity *[24]*, and volcanic deposition following megaflooding events *[10]* or intermittent between flooding events *[1]*.

Figure 1. MOLA colorized elevation map of Mangala Valles showing screenshot locations.

Evidence of Fluvial Activity

Figure 2. Examples of landforms interpreted to be the result of erosion by flooding:
A) Channel terraces, indicated by black arrows, and plucked floor, *P19_008474_1688_XN_11S150W, (149.79°W, 13.33°S)*;
B) Diverging linear ridges, *P05_002857_1629_XN_17S149W, (149.65°W, 17.40°S)*;
C) Converging streamlined ridges, *B02_010531_1704_XI_09S153W, (153.84°W, 9.18°S)*;
D) Streamlined island, *B02_010531_1704_XI_09S153W, (153.73°W, 9.50°S)*.

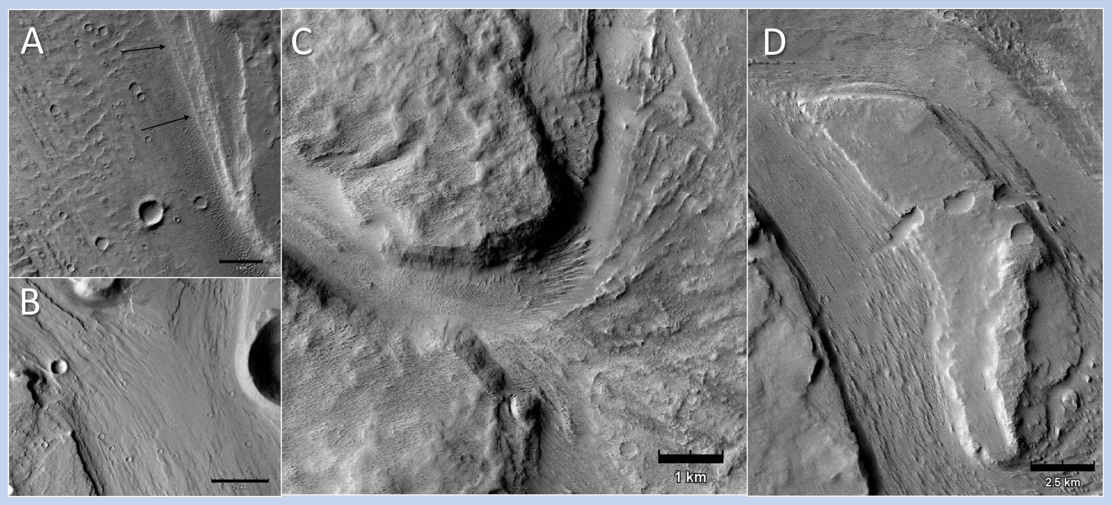

Context Camera [9]

Evidence of Volcanic Activity

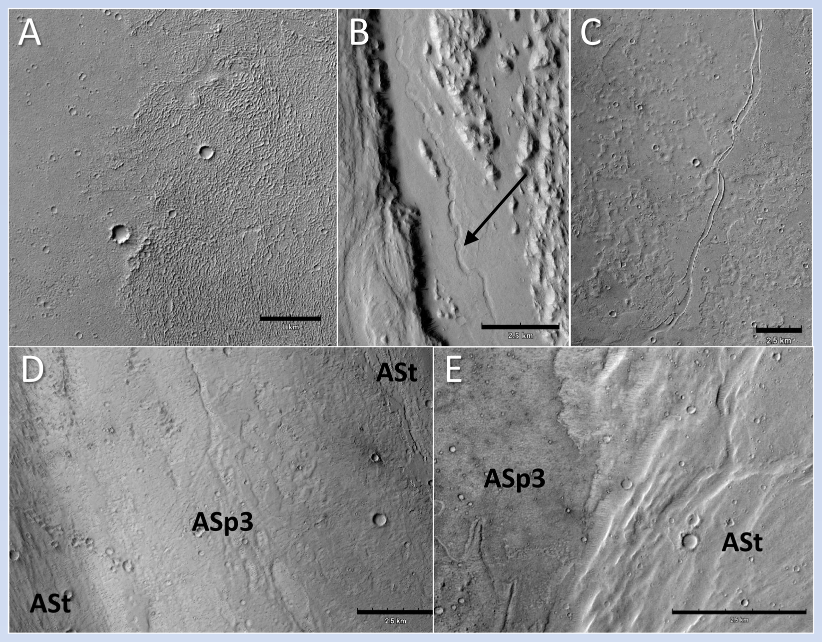

Figure 3. Examples of landforms interpreted to be the result of volcanic activity: A) Ridged flow margin, *G22_026816_1706_XN_09S153W, (152.84°W, 9.65°S)*; B) Lava tube collapse pits, indicated by black arrow, *P13_006114_1748_XN_05S151W, (151.01°W, 6.58°S)*; C) Sinuous lava channel, *G22_026829_1658_XN_14S147W, (148.6°W, 12.29°S)*; D) Muted topography and lava-rise pits flanked by fluvial ridges to the top right and bottom left, *P01_001591_1708_XN_09S151W (151.33°W, 11.35°S)*; E) Lobate margin overlaying fluvial ridges, *P05_002857_1629_XN_17S149W (149.30°W, 17.85°S)*.

Context Camera [9]

Evidence of Post-Emplacement Fluvial Modification of Volcanic Units

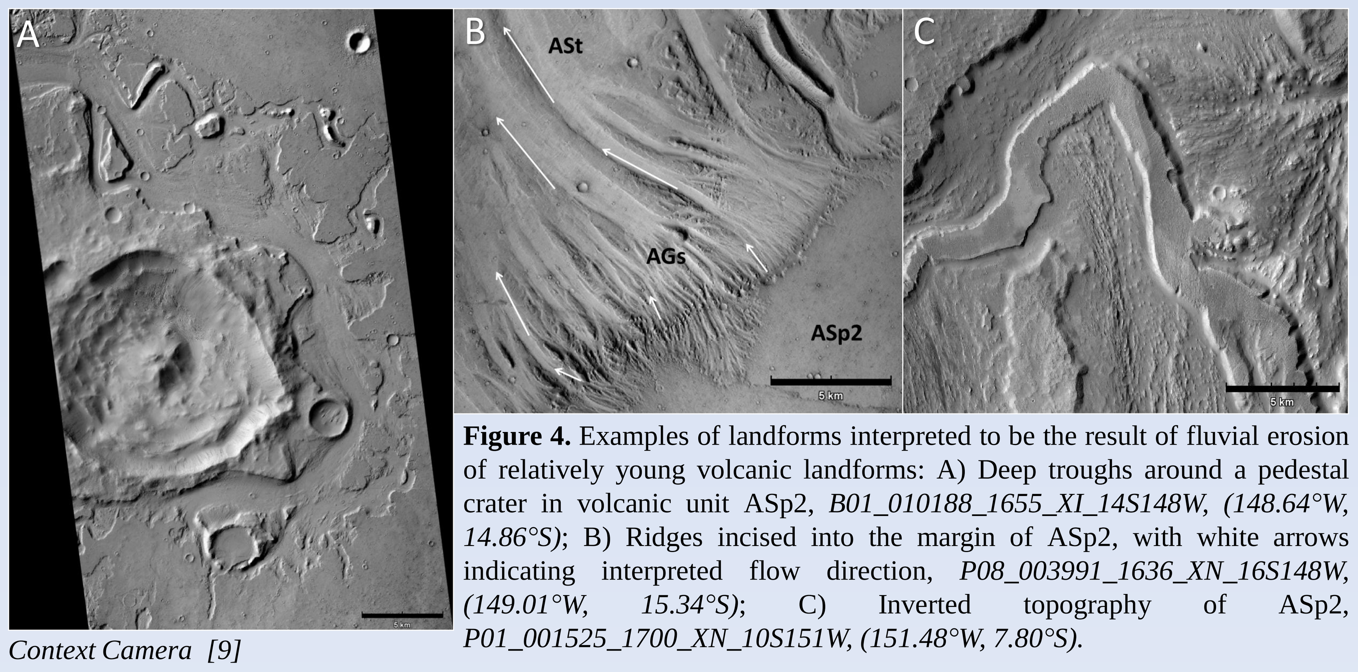

Figure 4. Examples of landforms interpreted to be the result of fluvial erosion of relatively young volcanic landforms: A) Deep troughs around a pedestal crater in volcanic unit ASp2, *B01_010188_1655_XI_14S148W, (148.64°W, 14.86°S)*; B) Ridges incised into the margin of ASp2, with white arrows indicating interpreted flow direction, *P08_003991_1636_XN_16S148W, (149.01°W, 15.34°S)*; C) Inverted topography of ASp2, *P01_001525_1700_XN_10S151W, (151.48°W, 7.80°S)*.

Context Camera [9]

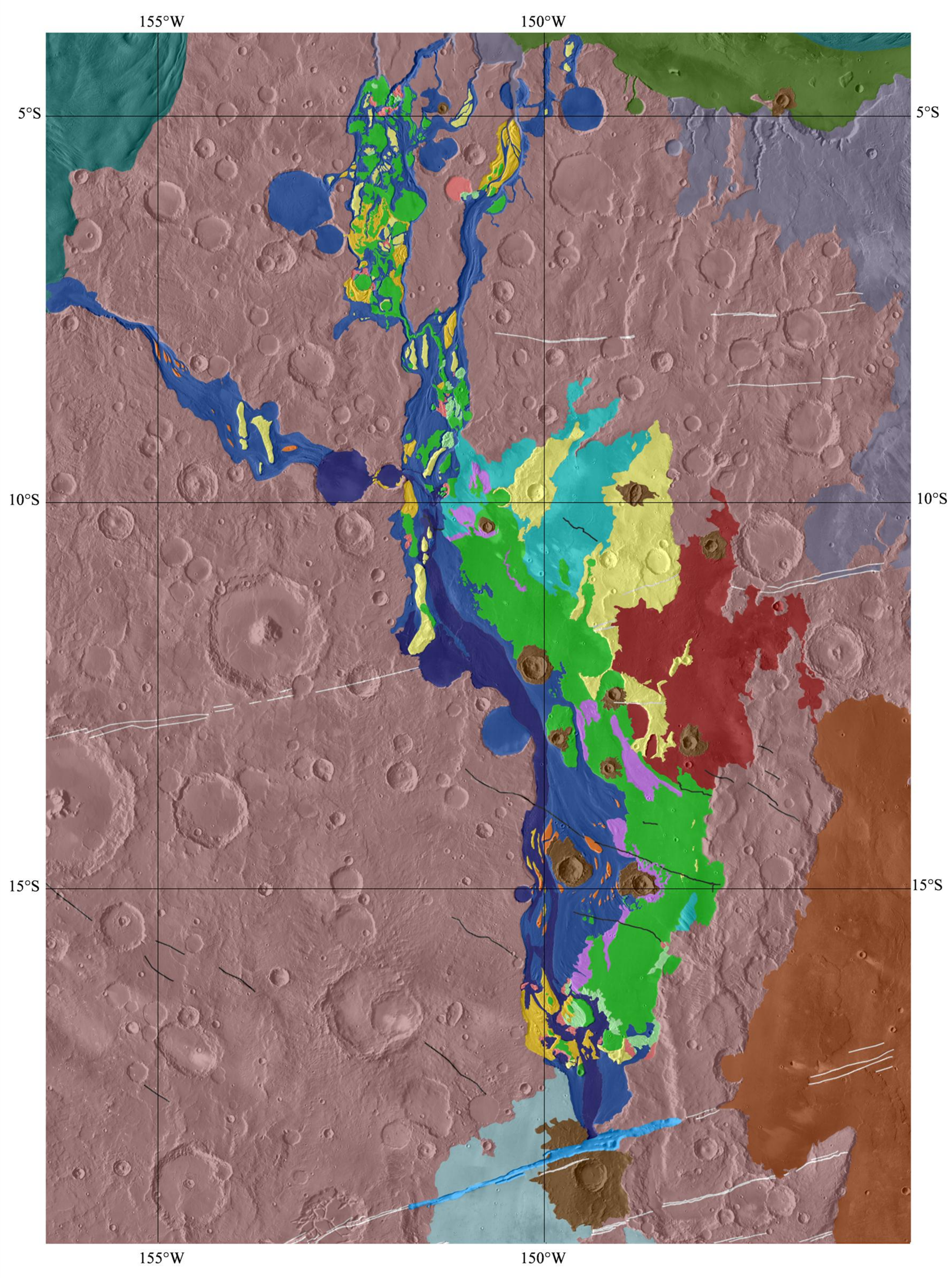

Legend

100 km

N W E S

Mangala Geomorphic Units

Smooth Plains 4 (ASp4). The flattest unit, with elevations ranging from about –75 m to –100 m. Extremely smooth with indistinct, flat interior lobes and muted craters. Extensive eolian activity. Image width 12 km (*CTX P13_006259_1680_XN_12S149W*).

Smooth Plains 3 (ASp3). Begins at –143 m elevation, increases mid–valley to –90 m, and then gradually decreases in elevation toward the north, terminating at a low of –800 m in the northwestern channel network. Anastomosing, smooth floor, lobate edges, landform embayment. Draped ridged topography. Image width 5.5 km (*CTX P01_001393_1655_XN_14S149W*).

Terraced Scoured (ATs). Appears predominantly as elongate islands appearing along the western edge of the valley within ASp3 and in the southern portion of Mangala Valles, confined to isolated high islands and terraces often capped by a small piece of ASp2. Bears a general scoured appearance, with deep linear grooves and steep walls. Image width 7 km *(CTX P16_007182_1626_XN_17S150W).*

Grooved Slope (AGs). Transitional from ASp2 to ASt. At the western margin of ASp2, deep, subparallel grooves originate with ridge orientations perpendicular to the margin of ASp2, where trough heads break up the edges of the plateau and form complex multitudes of narrow canyons, then curve to the north until aligned with ridges of ASt immediately to the west. Exposures heading in the interior of ASp2 are northwest–trending. Image width 9 km *(CTX P03_002079_1639_XN_16S149W).*

Polygonal Blocky (APb). Mapped in the southern valley and in the northern channels, appearing as low, subdivided smooth blocks with dissecting canyons off of the edges of ASp2 and ATs. They range in size from about 300 m to 3 km in width. Image width 4 km *(CTX P05_002857_1629_XN_17S149W).*

Small Knobbed (ASk). Appears in the southern portion of the valley and in the northern channels in small batches adjacent to APb, ATs, and ASp3. Knobs range 50–1500 m across and are rounder, more widely spaced, and generally more uniform in size than blocks of APb. Embayed by ASp3 in the southern valley. Image width 4.5 km *(CTX P05_002857_1629_XN_17S149W).*

Smooth Plains 2 (ASp2). Comprises the majority of the southeastern and middle portion of the valley and is scattered throughout the northern channels in disconnected islands of inverted topography. Smooth and flat, platey. Exhibits crater embayment, lobate margins, and streamlined features. Small bits of it appear on separate islands all throughout the valley, but most notably in the southern valley region and in the northern channels. Image width 11.5 km *(CTX P15_006760_1658_XN_14S148W).*

Large Knobbed (ALk). Rounded or plateaued islands with teardrop-shaped bars within the main central body and in the northwestern channel network of ASt. Plateaued islands are 150–300 m in height, rounded islands are <150 m in height. Image width 17 km *(CTX P14_006615_1645_XN_15S149W).*

Scoured Terrain (ASt). Subparallel linear grooves alternating with sharp ridges that circumvent obstacles, cut highland bedrock, and superpose other valley geomorphologies. Largely composed of vast networks of anastomosing channels with cutbank walls, channel terraces, and knobby streamlined islands with pendant bars scattered throughout. Image width 3 km *(HiRISE ESP_023783_1665_RED).*

Smooth Plains 1 (ASp1). Represents a topographic high of the valley, elevation range 100–450 m. Very flat along its northwestern geologic strike. Exhibits lobes, sinuous channels, pits, hummocky plains, rafts, and embayed and infilled impact craters. Often embays islands of HOt. Image width 4.5 km *(CTX G22_026829_1658_XN_14S147W).*

Old terrain (HOt). Partially resurfaced highland terrain. Exhibits high topographic variation and high crater densities. Often manifests as small islands between or within larger geological units. Tends to sit higher than the surroundings, with elevations approaching 500 m. Image width 3.5 km *(CTX P13_006259_1680_XN_12S149W).*

Adjacent Geologic Units

- **Medusae Fossae Fm, upper member (AMu)**
- **Medusae Fossae Fm, middle member (AMm)**
- **Plateau sequence, smooth unit (Hpl3)**
- **Tharsis lava flows (AHd1)**
- **Tharsis Montes Fm, member 3 (AHt3)**
- **Plateau sequence, cratered unit (NHpl1)**

Structures

- **Mangala Fossa**
- **Graben**
- **Pedestal crater**
- **Wrinkle ridge**

Interpreted Geologic History

*Note that earlier flooding phases are possible as well, the evidence for which has been subsequently erased.

Figure 5. Summary bar plot presenting crater retention model ages, grouped by geomorphic unit. Based on crater counts, stratigraphic relations, and differences in surface geomorphology, units ASp1, ASp2, and ASp3 are interpreted to be different aged volcanic units, and units ASt and AGs are interpreted to be fluvial, representative of two distinct flooding events. HOt is interpreted to be partially resurfaced Noachian Highlands, therefore the crater retention ages reported are likely an underestimate of the true age of highland bedrock.

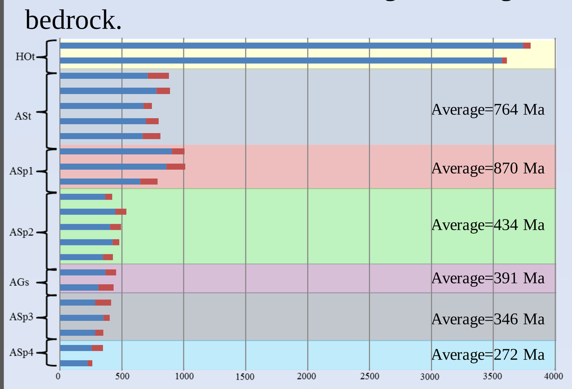

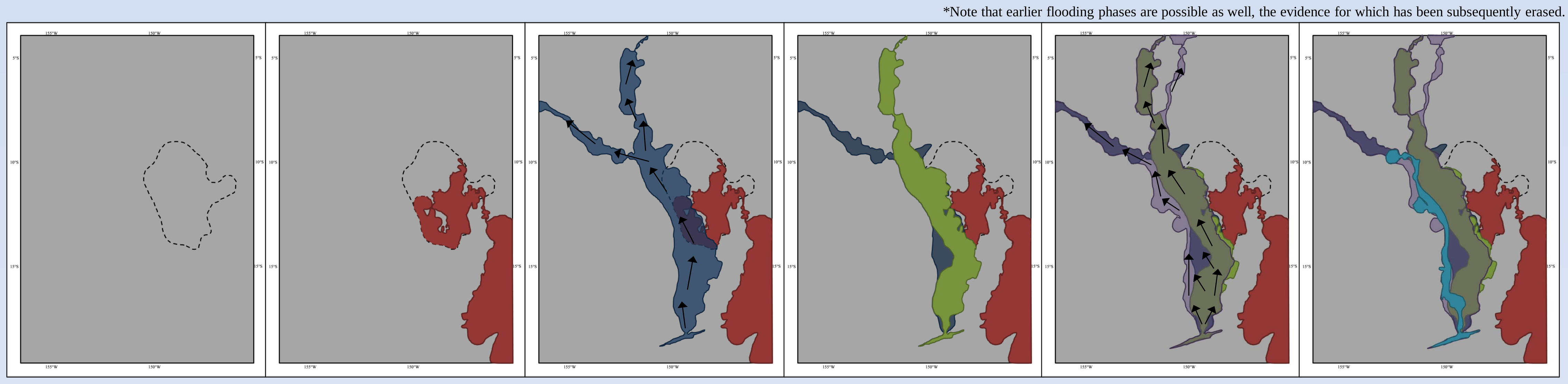

>1 Ga: A topographic low is produced by an unknown mechanism to an unknown extent, providing accommodation space for later basin fill.

700-1000 Ma: Deposition of Tharsis lava flows (solid red) from the northeast. The southern extent of these flows is unknown.

700-800 Ma*: Flooding and incision of Mangala Valles into highland bedrock, sourced at Mangala Fossa. Extent shown in transparent blue, arrows indicate flow direction.

400-500 Ma: Deposition of relatively young voluminous lava flows into the valles, sourced at Mangala Fossa (solid green).

~400 Ma: A second valley-carving flooding event that deepened and widened the valles toward the west and incised a third northern channel. Extent shown in transparent purple.

300-400 Ma: Emplacement of youngest volcanic units along the new topographic low to the west (solid light blue).

References: [1] Tanaka L. T. and Chapman M. G. (1990) *J. Geophys. Res.*, 95, B9, 14,315–14,323. [2] Zimbelman J. R. et al. (1992) *JGR*, 97, E11, 18,309–18,317. [3] Basilevsky A. T. et al. (2008) *Planet. Space Sci.*, 57, 917–943. [4] Ghatan G. J. et al. (2005) *EMP*, 96, 1–57. [5] Leverington D. W. (2011) *Geomorph.* 132, 51–75. [6] Leverington D. W. (2007) *JGR*, 112, E11. [7] Jaeger W. L. et al. (2010) *Icarus*, 205, 1, 230–243. [8] Chapman M. G. et al. (2010) *EPSL*, 294, 256–271. [9] Malin M. C. et al. (2007) *JGR*, 112, E5. [10] McEwen A. S. et al. (2012) *LPSC 2012*. [11] Smith D. E. et al. (2001) *JGR*, 106, E10, 23,689–23,722. [12] Christensen P. R. et al. (2004) *Space Sci. Rev.*, 110, 85–130. [13] Christensen P. R. et al. (2003) *Science*, 300, 5628, 2056–2061. [14] Christensen P. R. et al. (2009) *AGU 2009*. [15] McEwen A. S. et al. (2007) *JGR*, 112, 5. [16] Michael G. G. and Neukum G. (2010) *EPSL*, 294, 223–229. [17] Chapman M. G. et al. (1989) *USGS*. [18] Jaumann R. et al. (2007) *Planet. Space Sci.*, 55(7–8), 928–952. [19] Baker, V., Milton, D. (1974) *Icarus*, 23,27-41. [20] Sharp, R. P., Malin, M. C. (1975) *GSA Bulletin*, 86.5, 593. [21] Komar, P. (1979) *Icarus*, 37.1, 156-81. [22] McCauley, J. F. et al. (1972) *Icarus*, 17, 289-327. [23] Carr, M. H., Head, J. W. (2010) *EPSL*, 294, 185. [24] Head, J. W. (2004) *JGR*, 31, L10701.